AALBORG UNIVERSITY

DENMARK

Marine predator algorithm based PD-(1+PI) controller for frequency regulation in multi-microgrid system

Padhy, Sasmita; Sahu, Preeti Ranjan; Panda, Sidhartha; Padmanaban, Sanjeevikumar; Guerrero, Josep M.; Khan, Baseem

Document Version
Publisher's PDF, also known as Version of record

Link to publication from Aalborg University

ORIGINAL RESEARCH

Marine predator algorithm based PD-(1+PI) controller for frequency regulation in multi-microgrid system

Sasmita Padhy[1] | Preeti Ranjan Sahu[1] | Sidhartha Panda[2] |
Sanjeevikumar Padmanaban[3,4] (iD) | Josep M. Guerrero[5] | Baseem Khan[6] (iD)

[1]Department of Electrical Engineering, National Institute of Science and Technology (Autonomous), Berhampur, Odisha, India

[2]Department of Electrical and Electronics Engineering, Veer Surendra Sai University of Technology, Burla, Odisha, India

[3]Department of Electrical and Electronics Engineering, KPR Institute of Engineering and Technology, Tamil Nadu, India

[4]CTiF Global Capsule, Department of Business Development and Technology, Aarhus University, Aarhus, Denmark

[5]Center for Research on Microgrids (CROM), AAU Energy, Aalborg University, Aalborg, Denmark

[6]Department of Electrical and Computer Engineering, Hawassa University, Hawassa, Ethiopia

Correspondence
Baseem Khan, Department of Electrical and Computer Engineering, Hawassa University, Hawassa, Ethiopia.
Email: baseem.khan04@gmail.com

Abstract

Renewable generation uncertainty, dynamic load change, and system parameter variation play a significant role in the performance degradation of non-linear multi-microgrid (MMG) systems. As a result, intelligent control becomes the need of the hour for assisting superlative attribute- based consistent electric power. The application of marine predator algorithm (MPA)-based cascaded PD-(1+PI) controller for Automatic Generation Control (AGC) of MMG system is a novel work. A maiden attempt of the MPA is proposed to optimize the parameters of the cascaded PD-(1+PI) controller using the integral time absolute error criterion. To demonstrate its superiority, the proposed algorithm is compared to the genetic algorithm, differential evolution, and grey wolf optimization. MPA then applied to conventional controller PID, cascaded PD-PI controller and proposed PD-(1+PI) controller for frequency control in multi-microgrid system. The robustness of the suggested controller is verified over PID and PD-PI controller by taking step and random load perturbation and integrating the renewable sources like solar and wind with their uncertain nature. The simulation of the investigated interconnected microgrid is carried out in MATLAB/SIMULINK environment. Finally, detailed simulation and hardware in the loop experimental results are presented to confirm the practicality of the proposed approach.

1 | INTRODUCTION

In the recent days the demand of electric power increases with the increase in population and increase in industries worldwide. So, the fossil fuel is getting ended in fulfilling the increased demand of the public, industry etc. In light of this the renewable sources are used and microgrid concept can be introduced [1]. A microgrid is one which contains distributed energy resources, storage devices, residential and commercial loads, centralized and decentralised controllers [2]. The unpredictable nature of renewable sources, inertia less power converters, and sudden change in the load perturbation causes frequency instability in the microgrid [3]. To ensure the quality power from microgrid proper control is needed. The main responsibility of the secondary control in microgrid is to restore the frequency and enhance the power quality [4]. The second step is to create and maintain synchronisation between the utility grid and the microgrid. In addition, optimum operation of the microgrid can be achieved [5, 6]. Microgrid operates in two modes, that is, grid connected mode and islanded mode. The distribution network is split in to small microgrid regions to form the multi-microgrid (MMG) system because of the advantages of microgrid [7]. The features like flexibility towards disturbance, intentional islanding and self-repair motivates for formation of MMG system. The interconnection in microgrids causes the sharing of extra power but at the same time makes the system more complicated to control. Because of the stochastic nature of the renewable sources and random disturbances of load in MMG system the frequency deviation and tie-line power deviation will more which may make the system unstable. To obtain a

persistent and persuasive behaviour in the MMG system secondary controller is needed which can restore the steady-state in the system. To control load frequency deviations, several strategies in various domains of control systems have been used, including decentralized control, robust control, inequalities in linear matrix, internal model control, adaptive control, sliding mode control, and intelligent control [8]. Traditional PID controllers appear to operate well in set point tracking and disturbance rejection applications, according to the research. For a wide range of working situations for stable, unstable, and non-linear processes, this controller provides an optimized and durable display.

1.1 | Literature survey

The literature contains both conventional and artificial intelligence-based solutions for solving the load frequency control (LFC) problem [9]. The authors in [10] presented Ziegler-Nichols-based Controller for parameters tuning of PID controller, while authors in [11–13] proposed a traditional PI controller-based approach. In [14], the author proposes a hybrid system that includes diesel engine generator, wind turbine generator, fuel cell, and acqa-electrolyzer. The authors in [15] presented an internal model-based LFC. In the literature, swarm intelligence-based approaches have been used to tune PID gains, such as the Moth-Flame optimised fuzzy PID controller proposed in [16]. The authors employed a biogeography-based optimization technique in his paper [17]. Grey wolf optimization for Automatic Generation Control of a two-area interconnected power system with only thermal units presented in [18]. In [19], the author presented gravitational search algorithm based PIDF strategy. Differential search algorithm tuned PID/PIDF controller design discussed in [20]. The author discussed about imperialist competitive algorithm optimized conventional and fuzzy logic control strategy [21]. In [22], the author proposed FTIDF controller tuned by competition over resources algorithm. The author discussed in [23] about cascaded controller optimized by using Imperialist competitive algorithm. The author employed genetic algorithm for load frequency control of a MMG system discussed in [24]. The author presented modified equilibrium optimizer tuned type-2 fuzzy PID controller for hybrid power system in [25]. In [26], the author proposed PD-PID controller using sine cosine algorithm for hybrid system. The authors presented gravitational search algorithm optimized PI controller for multi-area power system in [27]. The author investigates an imperialist competition algorithm optimized FPIDF-(1+PI) [28] and FPIDN-FOPIDN controller [29]. In [30], an ICA tuned C-$I^\lambda D^\mu N$ controller is used for hydro thermal system considering RES. The authors proposed a COA optimized $FPI^\lambda DF$ controller in a two-area system incorporating wind turbine [31]. The authors presented a dragonfly search algorithm optimized (1+PD)-PID cascade controller for two-area thermal system [32]. In [33], the authors discussed the performance analysis of optimal controller using various intelligent techniques for multi area system considering system non-linearities. The authors investigate the modified Jaya

algorithm optimized controller parameters for wind integrated power system [34]. The author designed an improved gravitational search algorithm optimized AFFFOPID controller for pumped storage hydro unit [35]. The author utilized a GA tuned IPD controller for hybrid power system considering renewable energy [36].

1.2 | Research gap and motivation

Some recent literatures for the classical controllers like I controller, PI controller and PID controller are working adequately for hybrid microgrids. But these controllers may cause sluggish operation during sudden load disturbance or parametric variation; there are sliding mode controller, fractional order PID and PI controllers used in microgrid after series of research. It may enhance the complexity in the structure and cost. The cascaded structure like PI-PD controller's predominance over PID controller is verified in the literature. These works motivate to suggest a cascaded PD-PI controller with a forward path in PI controller and to investigate its effect on the dynamics of MMG system. The suggested controller with inner and outer loop processes the frequency error signal. Initially processed by inner loop and then it gets passed to outer loop.

Inspired from the literature, the paper suggests a novel cascaded PD-PI controller with a unit forward path in parallel with PI controller to improve the dynamic characteristics of the MMG system. The parameters of the recommended controller are tuned by a recently published algorithm named Marine Predators Algorithm (MPA) [37] which converges at global minima instead of getting trapped at local minima. It outperforms various meta-heuristic algorithms in terms of convergence to the best result, parametric variation etc.

1.3 | Contribution and paper organization

The main contributions of this paper are summarized as follows:

1. A novel Marine Predator Algorithm based PD-1+PI (Cascaded PD- PI controller with forward path) has been proposed in LFC of two area microgrid.
2. The superiority of MPA is verified over GA, DE, and GWO in terms of minimum error, and dynamic response.
3. Design a cascaded PD-(1+PI) controller to verify its supremacy over PID and PD-PI controller in LFC of two area MMG system.
4. To verify the effectiveness and robustness of the proposed controller, different types of disturbance like step load and random load perturbation are included in MMG system.
5. To demonstrate the efficiency of the proposed method the system is projected with probabilistic behaviour of the renewable sources.
6. An OPAL-RT OP5700 real-time simulator has been used to validate simulation results.
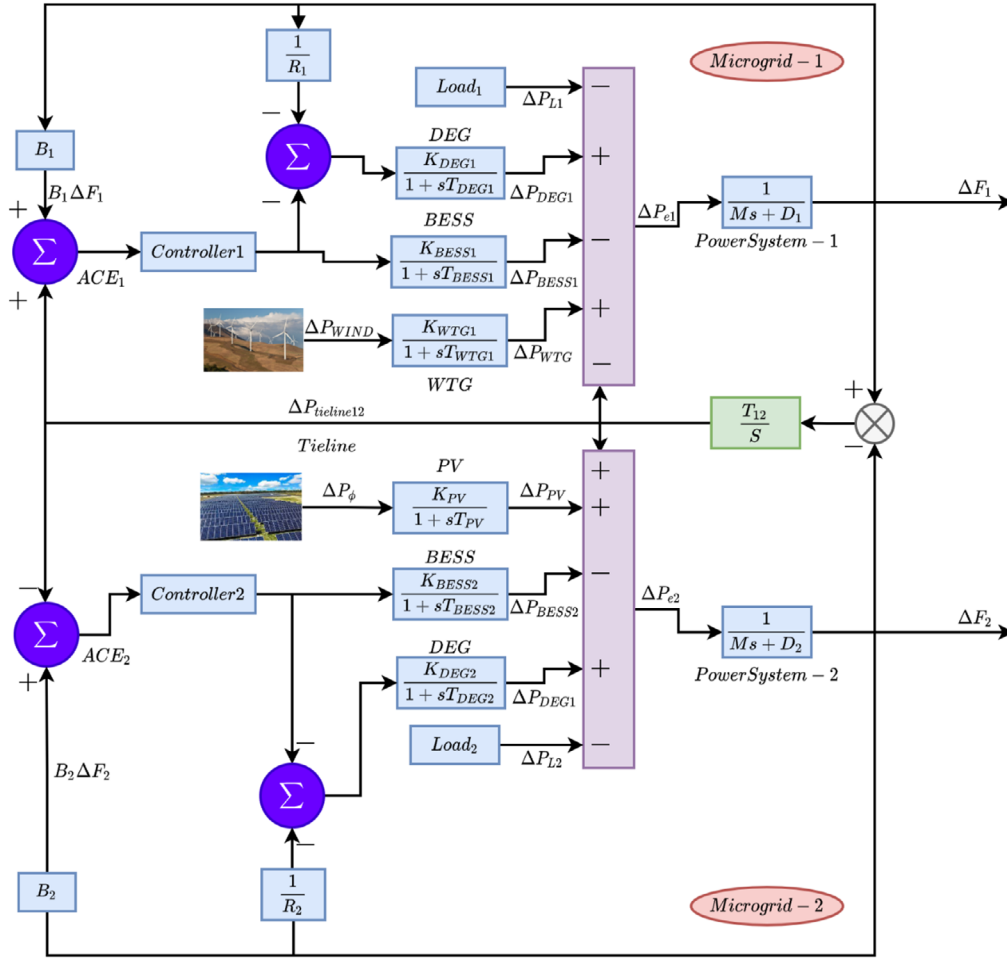
FIGURE 1   Transfer function model of proposed multi-microgrid system

2 | MODELING OF MULTI-MICROGRID (MMG) SYSTEM

The proposed transfer function model of proposed MMG system is shown in Figure 1 and schematic diagram of the proposed MMG system is shown in Figure 2. The investigated system is a MMG system consisting of two microgrids which are connected through tie-line. Microgrid-1 consists of wind turbine, Diesel engine generator (DEG) and battery energy storage system (BESS) and the microgrid-2 consists of solar PV cell, BESS and DEG along with PD-(1+PI) controller in each microgrid. For the stable operation of power system, the generated power should be equal to demand power. The wind turbine in microgrid-1 and PV solar cell in microgrid-2 cannot generate constant power all the time because of the unpredictable nature. That situation creates a gap between generation and demand and can be fulfilled by the storage units present in the microgrids. In this paper the proposed controller PD-(1+PI) gives the control signal to the BESS and DEG to maintain the power and reduce the gap in the power. Further the proposed controller helps in minimizing the frequency deviation and oscillations in tie line power.

2.1 | Modelling of wind turbine generator

Power generated by the wind turbine depends upon the base speed and noise speed of turbine. It has gust speed and ramp speed too.

Base fluctuation in base speed can be represented by:

$$V_{WB} = C = 7.5H(t) + 4.5H(t-5) - 2H(t-15) \quad (1)$$

Randomness in noise speed can be represented by a step function:

$$V_{WN} = 2\sigma^2 \sum_{i=1}^{n} \sqrt{SV(\omega i)\Delta\omega}\, cos(\omega it + \varphi i) \quad (2)$$

$\Delta\omega = 0.5 - 2$ rad/s, $\sigma^2 = 200$ (variance noise component), $SV(\omega i)$ is the spectral density function, and $n = 50$.

In terms of wind speed, wind power is expressed as:

$$P_w = \frac{1}{2}\rho AC_P V_w^3 \quad (3)$$
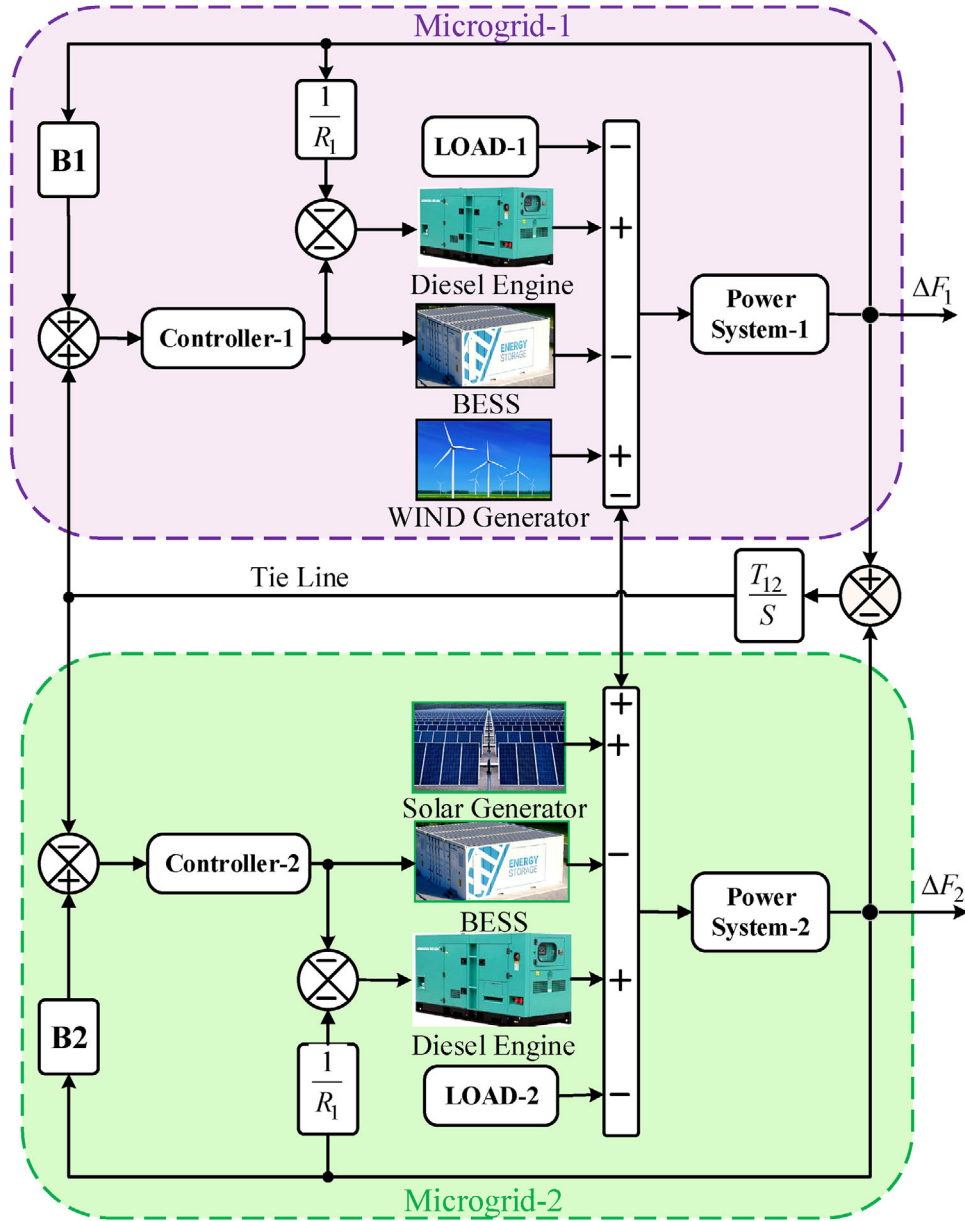
FIGURE 2 Proposed multi-microgrid system

where, ρ is air density, A is swept area of blades and C_p represents the power coefficient.

$$G_{WTG} = \frac{K_{WTG}}{1 + sT_{WTG}} = \frac{P_{WTG}}{P_W} \quad (4)$$

2.2 | Modelling of photovoltaic (PV) cell

The examined PV system's output power (in watts) is determined by:

$$P_{PV} = \eta S \phi \{1 - 0.005 (T_a + 25)\} \quad (5)$$

where η ranging from 10% is the PV array conversion efficiency, $S = 4084 \text{ m}^2$ is the measured area of the PV array, $\Phi = 3 \text{ kW/m}^2$ is the solar radiation, and T_a is ambient temperature in degree Celsius. Because η and S are constant the value of P_{PV} is determined by T_a and Φ. Here, T_a is fixed at 25°C in this study while P_{PV} is linearly varied with Φ only.

$$\varphi = 0.52H(t) - 0.032H(t-10) + 0.079H(t-20) + \varphi n(t) \quad (6)$$

where φn is the solar radiation's stochastic component in the range (0.1, 0.1). The transfer function of $_{SPV}$ is represented by linear first order.

$$G_{SPV}(s) = \frac{K_{PV}}{1 + sT_{PV}} \quad (7)$$

2.3 | Diesel engine generator

The DEG can provide deficit power in order to reduce the power gap between demand and supply. It is a non-linear element as it has generation restrictions. Its transfer function is given as:

$$G_{DEG}(s) = \frac{K_{DEG}}{1 + sT_{DEG}} = \frac{\Delta P_{DEG}}{\Delta U} \quad (8)$$

The controller output signal controls the energy storage devices. They act as sources or loads in the system depending on the situation. They contain rate restrictions that allow the elements to operate in the nonlinear domain. Furthermore, rate constraints aid in dealing with the devices electromechanical characteristics and minimise mechanical damage caused by rapid frequency fluctuations.

The transfer function of the BESS is given as:

$$G_{BESS} = \frac{K_{BESS}}{1 + sT_{BESS}} = \frac{\Delta P_{BESS}}{\Delta U} \quad (9)$$

2.4 | Power system modelling

With a change in power (ΔP) as an input and a change in frequency (Δf) as an output, the dynamics of the power system are given by:

$$G(s) = \frac{\Delta f}{\Delta P} = \frac{1}{D + Ms} \quad (10)$$

In (10), $D = 0.12$ and is the damping parameter while $M = 0.2$ is the inertia parameter of the MMG system.

3 | PROPOSED PD-(1+PI) STRUCTURE

When there is a change in input to the controller the control signal to the plant changes abruptly. The output of the controller may lead to deterioration of transient response of the system. So, to prevail over the disadvantage of PID controller a new structure in the controller has been proposed in the present study.

PD-(1+PI) controller is one which is a simple cascade PD-PI controller with a unit forward path in parallel with PI controller. Here the proposed PD-(1+PI) controller structure detailed in Figure 3. The input to the controller is area control error (ACE). In MMG, ACE is the result of combining frequency deviation and tie-line power in a predictable manner.

$$ACE_1 = B_1 \Delta F_1 + \Delta P_{tieline12} \quad (11)$$

$$ACE_2 = B_2 \Delta F_2 + \Delta P_{tieline21} \quad (12)$$

As PD controller is in cascade with (1+PI) controller there are more than one tuning hubs to tune the controller parameter so it has better chance of improving the dynamic characteristics and the sluggish response will be improved which is because of the controllers involving integral controller. In the proposed controller the output of PD controller will act as the input to the (1+PI) controller.

$$O_{PD} = (KP_i + KD_i s) ACE_i \quad (13)$$

$$O_C = O_{PD} \left(1 + KP_{ii} + \frac{KI_i}{s} \right) \quad (14)$$

O_{PD} is the output of PD controller and O_C is the output of (1+PI) controller. Similar controller is designed for each microgrid in MMG system. To get the desired output of the controller and to have greater impact of controller on the system response, the parameters of PD-(1+PI) controller are tuned using a recent optimization technique named marine predator algorithm.

3.1 | Problem formulation

The objective function is to minimize frequency fluctuation in each microgrid and tie-line power fluctuation, which can be represented by Integral time absolute error (ITAE).

$$J = \int_0^t (|\Delta F_1| + |\Delta F_2| + |\Delta P_{tie}|) t dt \quad (15)$$

The MPA algorithm is utilized to tune the parameters of PD-(1+PI) controller and to obtain the minimum values of frequency and tie-line power fluctuation. These minimum values will help in efficient performance of MMG system.

4 | MARINE PREDATOR ALGORITHM (MPA)

The Marine Predator Algorithm (MPA), which is a population-based technique and is supported by the survival of the fittest method, is one of the newly proposed optimization techniques [37]. The MPA is divided into three phases:

In the early iterations of the optimization process, a high velocity ratio arises when the prey's velocity is more than the predator's velocity.

In the midst of the optimization phase, the velocity of prey and predators is equal, resulting in a unity velocity ratio.

In the last stages of the optimization process, a low velocity ratio occurs when the prey's velocity is lower than the predator's velocity.

Initial solution is specified by:
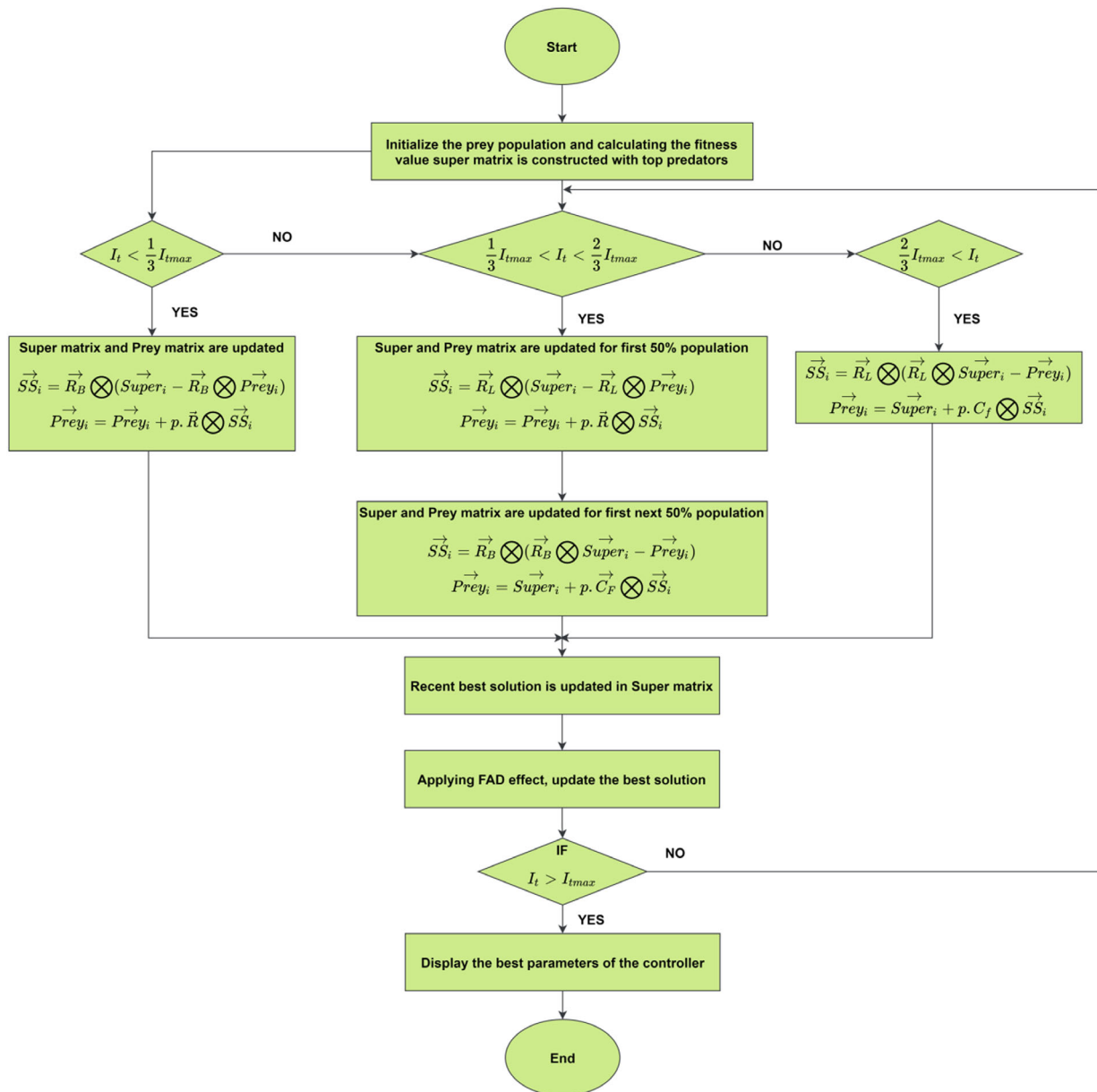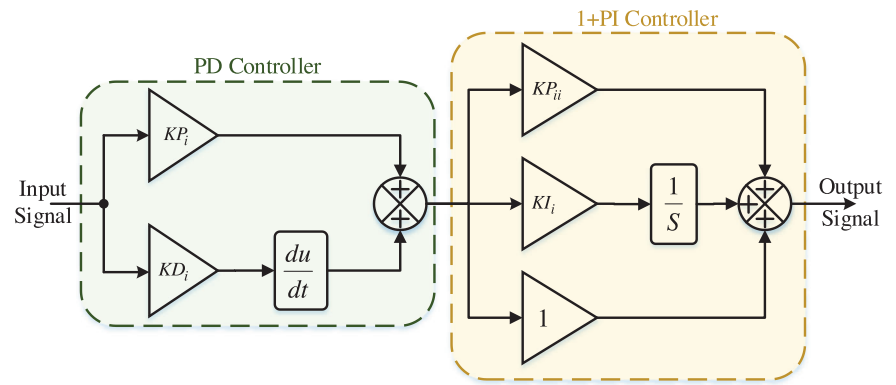
$$Y_0 = Y_{min} + rand(Y_{max} - Y_{min}) \quad (16)$$

FIGURE 3   Proposed PD-(1+PI) structure

FIGURE 4   Flow chart of the proposed MPA

TABLE 1 Optimized parameters of various controllers PID/PD-PI/PD-(1+PI) with GA/DE/GWO/MPA for case 3

Controller gain		PID controller				PD-PI controller				PD-(1+PI) controller			
		GA	DE	GWO	MPA	GA	DE	GWO	MPA	GA	DE	GWO	MPA
Area 1	KP1	1.971	1.373	2.001	1.943	1.581	1.874	2.000	1.990	1.881	1.651	1.999	1.989
	KI1	1.269	1.700	1.989	1.988	1.844	1.111	2.000	1.980	1.419	1.690	1.989	1.987
	KD1	1.2545	0.862	1.046	1.356	0.3117	0.471	1.713	1.986	0.992	0.398	1.903	1.983
	KP11	___	____	___	___	1.9900	1.3022	1.2110	1.9422	0.5466	1.546	0.147	0.601
A rea 2	KP2	0.378	1.714	1.990	1.959	1.919	1.894	1.9496	1.9852	1.3764	1.5246	1.9060	1.9895
	KI2	0.847	1.923	2.010	1.982	1.014	1.845	1.9864	1.9900	1.5229	1.5149	2.000	1.9900
	KD2	0.076	1.196	0.450	0.376	1.211	1.899	1.9429	1.9679	0.3617	0.7194	1.6058	1.9893
	KP22	___	____	___	___	1.238	0.709	0.7539	1.9900	1.4953	1.1411	1.9300	1.8425
ITAE		8.894	7.942	7.8577	7.8135	5.726	5.567	3.0357	2.9712	4.761	4.7160	2.884	2.629

TABLE 2 System's transient response parameters utilising a PID controller with the GA/DE/GWO/MPA Algorithm (under case 1)

Studied controller	Transient response parameters									ITAE
	Undershoot (p.u)			Overshoot (p.u)			Settling time (s)			
	ΔF_1	ΔF_2	ΔP_{tie}	ΔF_1	ΔF_2	ΔP_{tie}	ΔF_1	ΔF_2	ΔP_{tie}	
	$\times 10^{-3}$	$\times 10^{-3}$	$\times 10^{-3}$	$\times 10^{-3}$	$\times 10^{-3}$	$\times 10^{-3}$				
GA PID	6.6	13.7	63.4	8.6	38.2	3.7	8.5	7	12.79	0.862
DE PID	14.9	13.1	23.5	8.042	28.5	0.9	6.5	6.6	11.25	0.353
GWO PID	7.91	2.6	22.7	5.124	7.11	0.48	5.7	5.7	10.91	0.349
MPA PID	6.4	6.6	20.5	4.56	8.96	0.4	5	5.5	10.72	0.332

TABLE 3 System's transient response parameters under investigation involving PD-PI controller with GA/DE/GWO/MPA Algorithm (under case 1)

Studied controller	Transient response parameters									ITAE
	Undershoot (p.u)			Overshoot (p.u)			Settling time (s)			
	ΔF_1	ΔF_2	ΔP_{tie}	ΔF_1	ΔF_2	ΔP_{tie}	ΔF_1	ΔF_2	ΔP_{tie}	
	$\times 10^{-3}$	$\times 10^{-3}$	$\times 10^{-3}$	$\times 10^{-3}$	$\times 10^{-3}$	$\times 10^{-3}$				
GA PD-PI	−11.3	−2.9	−18	3.33	4.63	0	8.1	10.5	8.65	0.4956
DE PD-PI	−3.9	−2.87	−10.12	2.02	3.64	0	6.5	6.44	15.14	0.1626
GWO PD-PI	−3.01	−2.59	−9.37	1.40	3.25	0	4.6	5.28	8.73	0.1798
MPA PD-PI	−2.33	−1.05	−7.57	1.30	1.99	0	4.23	4.21	8.6	0.1385

It is evenly dispersed throughout the search space. As a result, the prey and predator are separated by a greater distance, and the prey uses the Brownian moment to explore the search space. For the variables, Y_{max} is the maximum value and Y_{min} is the minimum value. With top predators assigned to reproduce m times, a super matrix is generated.

$$Super = \left[Y^l_{1,1} Y^l_{1,2} \dots Y^l_{1,D}; Y^l_{2,1} Y^l_{2,2} \dots Y^l_{2,D}; Y^l_{M,1} Y^l_{M,2} \dots Y^l_{M,D} \right]$$

(17)

The number of variables is M, and the dimension is D. The Prey matrix has the same dimensions as the Super matrix and is determined by:

$$Prey = \left[Y_{1,1} Y_{1,2} \dots Y_{1,D}; Y_{2,1} Y_{2,2} \dots Y_{2,D}; Y_{M,1} Y_{M,2} \dots Y_{M,D} \right]$$

(18)

The predator finds itself and constructs the Super Matrix based on the location of prey. In the stage where high velocity ratio is kept.
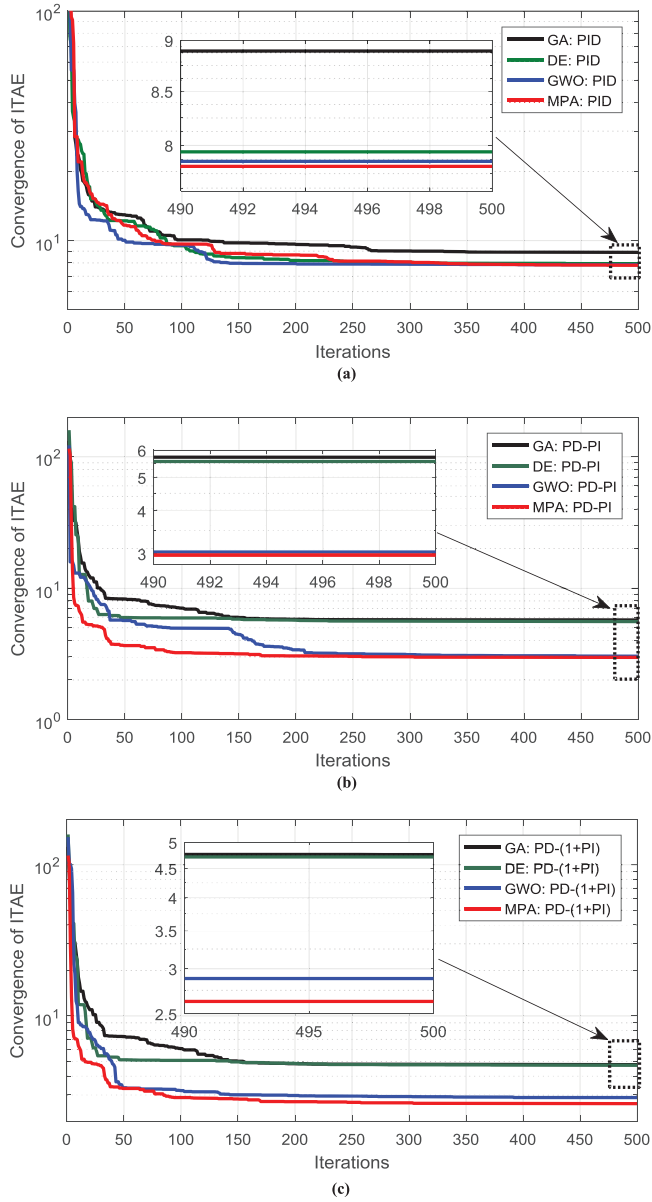
FIGURE 5 Comparison of MPA convergence characteristics with other optimization techniques (a) PID controller (b) PD-PI controller (c) Proposed PD-(1+PI) controller
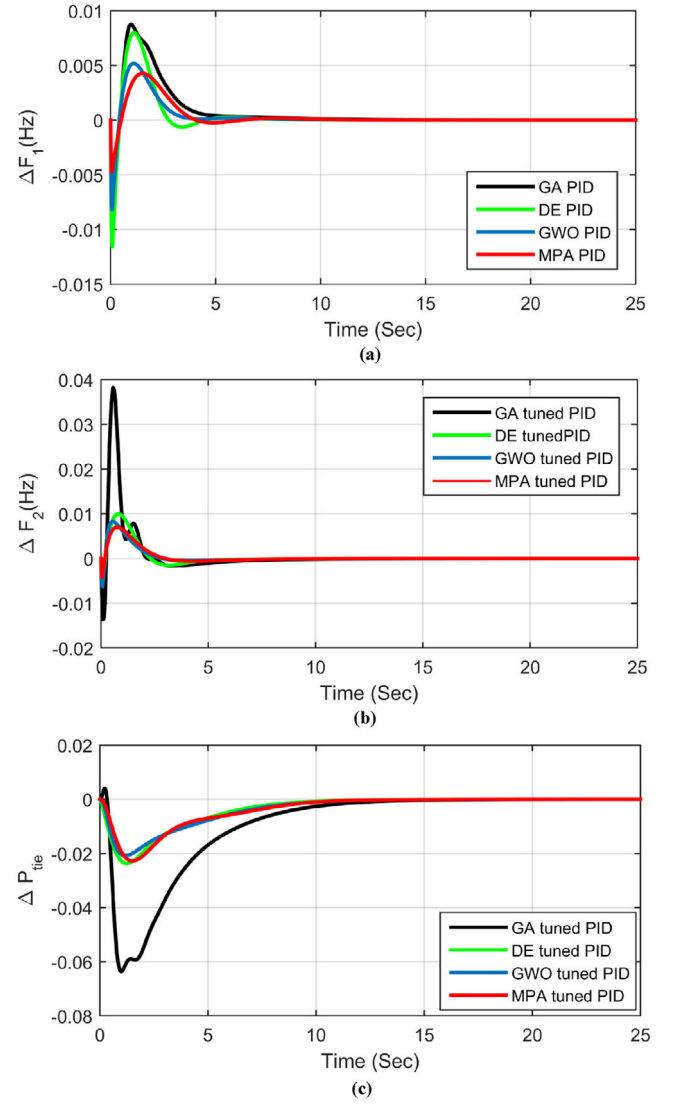

FIGURE 6 ynami MMG's Dynamic response comparison under case 1 (MPA/GA/DE/GWO) with PID controller (a) ΔF_1 in microgrid-1 (b) ΔF_2 in microgrid-2 (c) ΔP_{tie}

4.1 | Step where unity velocity is maintained

For $1/3\, I_{tmax} < I_t < 2/3 I_{tmax}$
For the first half of the population:

$$\vec{SS_i} = \vec{R_L} \otimes (\overrightarrow{Super_i} - \vec{R_L} \otimes \overrightarrow{Prey_i}) \qquad (21)$$

$$\overrightarrow{\Pr ey_i} = \overrightarrow{\Pr ey_i} + p.\vec{R} \otimes \vec{SS_i} \qquad (22)$$

And in the next 50% of population:

$$\vec{SS_i} = \vec{R_B} \otimes (\vec{R_B} \otimes \overrightarrow{Super_i} - \overrightarrow{Prey_i}) \qquad (23)$$

$$\overrightarrow{\Pr ey_i} = \overrightarrow{Super_i} + p.C_F \otimes \vec{SS_i} \qquad (24)$$

For $I_t < 1/3\, I_{tmax}$

$$\vec{SS_i} = \vec{R_B} \otimes \left(\overrightarrow{Super_i} - \vec{R_B} \otimes \overrightarrow{Prey_i} \right) \qquad (19)$$

$$\overrightarrow{\Pr ey_i} = \overrightarrow{\Pr ey_i} + p.\vec{R} \otimes \vec{SS_i} \qquad (20)$$

As the prey follows the levy movement and the predator follows the Brownian moment, this stage involves both exploration and exploitation.
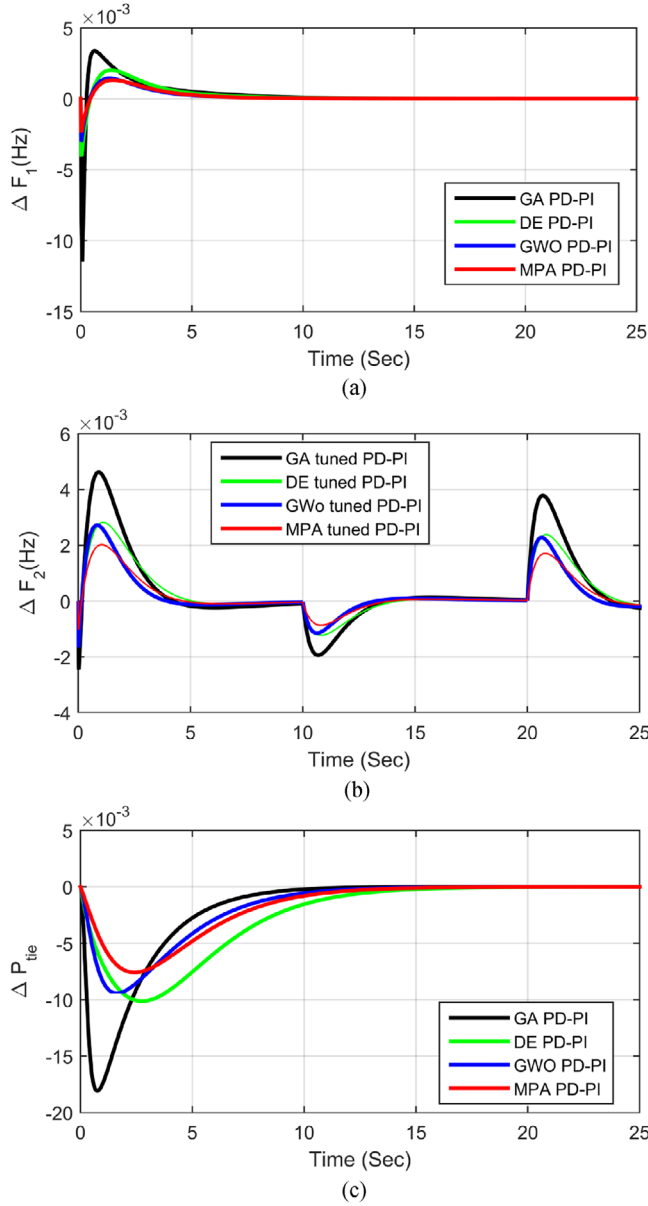
FIGURE 7 ynami MMG's dynamic response comparison under case 1 (MPA/ GA/DE/GWO) with PD-PI controller (a) ΔF_1 in microgrid-1 (b) ΔF_2 in microgrid-2 (c) ΔP_{tie}
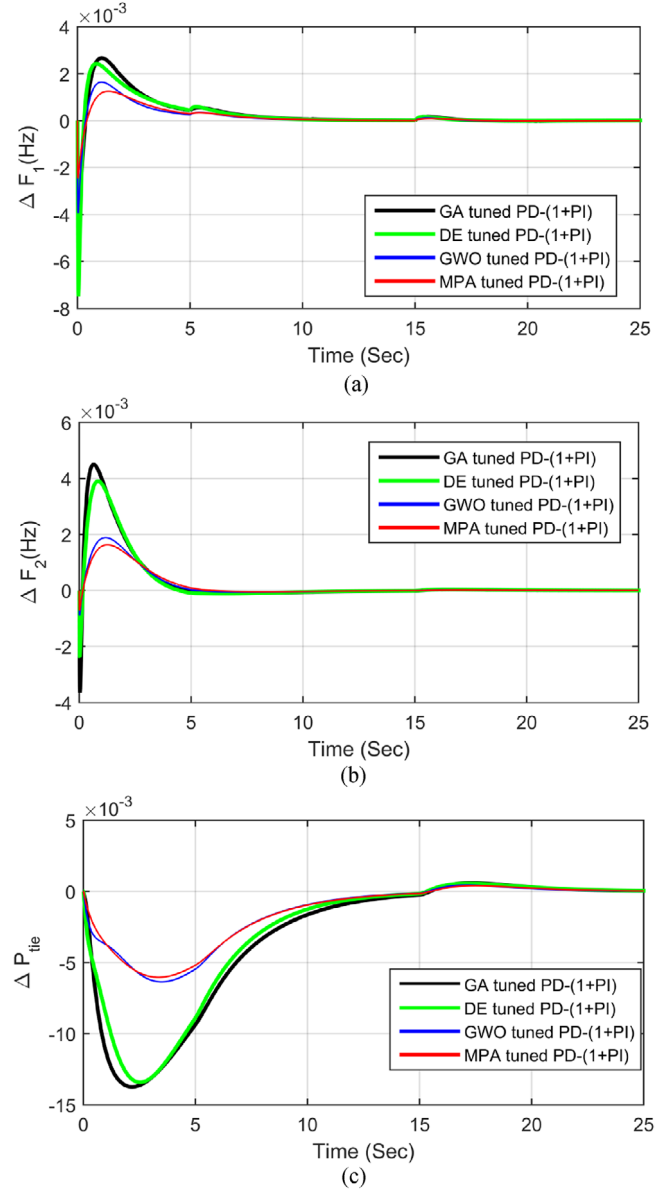
FIGURE 8 ynami MMG's dynamic response comparison under case 1 (MPA/GA/DE/GWO) with proposed PD-(1+PI) Controller (a) ΔF_1 in microgrid 1(b) ΔF_2 in microgrid 2 (c) ΔP_{tie}

$$C_F = \left(1 - \frac{I_t}{I_{t\,max}}\right)^{\left(2\frac{I_t}{I_{t\,max}}\right)} \qquad (25)$$

Finally, the equations for the stage where a low velocity ratio is maintained are as follows:

For $I_t > 2/3 I_{tmax}$

$$\overrightarrow{SS_i} = \overrightarrow{R_L} \otimes (\overrightarrow{R_L} \otimes \overrightarrow{Super_i} - \overrightarrow{Prey_i}) \qquad (26)$$

$$\overrightarrow{Prey_i} = \overrightarrow{Super_i} + p.C_F \otimes \overrightarrow{SS_i} \qquad (27)$$

The behaviour of the predator's changes due to fish aggregating devices (FAD) effect. Sharks spend more than 80% of their time in close proximity to FAD, and the remaining 20% will likely take a longer jump in various dimensions to reach an environment with a different prey distribution [38]. These are the local optimum points and its effect as getting trapped at these points. The long jumps performed by the predator allow it not to get trapped at the local optimum points. Predator its value is taken as 0.2 in the proposed algorithm.

The number of search agents and iterations may vary depending on the application. The number of search agents in the current study is 30. The chosen number of iterations is 500, which will shorten the assessment time. The flow chart of the proposed MPA is displayed in the Figure 4.

TABLE 4 System's transient response parameters under investigation involving PD-(1+PI) controller with MPA/ GA/DE/GWO Algorithm (under case 1)

Studied controller	Transient response parameters									ITAE
	Undershoot (p.u)			Overshoot (p.u)			Settling time (s)			
	ΔF_1 $\times 10^{-3}$	ΔF_2 $\times 10^{-3}$	ΔP_{tie} $\times 10^{-3}$	ΔF_1 $\times 10^{-3}$	ΔF_2 $\times 10^{-3}$	ΔP_{tie} $\times 10^{-3}$	ΔF_1	ΔF_2	ΔP_{tie}	
GA PD-(1+PI)	7.29	3.64	13.74	2.65	4.48	0.576	9.3	4.52	23.5	0.0432
DEPD-(1+PI)	7.26	2.36	13.42	2.40	3.90	0.542	9.24	4.46	21.2	0.0387
GWO PD-(1+PI)	3.88	0.89	6.35	1.63	1.88	0.425	8.12	4.41	18.3	0.0239
MPA PD-(1+PI)	2.4	0.63	6.03	1.21	1.62	0.381	7.71	4.36	18.1	0.0232

TABLE 5 Transient response parameters of PID/PD-PI /PD-(1+PI) controllers tuned with MPA technique under case 2

Disturbance	Controller	System's transient response parameters									ITAE
		Undershoot (p.u)			Overshoot (p.u)			Settling time (s)			
		ΔF_1 $\times 10^{-3}$	ΔF_2 $\times 10^{-3}$	ΔP_{tie} $\times 10^{-3}$	ΔF_1 $\times 10^{-3}$	ΔF_2 $\times 10^{-3}$	ΔP_{tie} $\times 10^{-3}$	ΔF_1	ΔF_2	ΔP_{tie}	
At $t = 0$ SLP $= 0.1$	MPA PID	−4.32	−4.183	−22.2	4.109	6.89	1.099	18.23	6.397	19.82	0.416
At $t = 5$ s $\Delta V_w = 3$ m/s	MPA PD-PI	−3.46	−1.078	−6.597	1.608	2.084	0.459	10.91	5.492	19.48	0.259
At $t = 15$ s $\Delta V_w = 2$ m/s	MPA PD-(1+PI)	−2.30	−0.567	−5.751	1.244	1.597	0.230	8.75	4.937	15.08	0.239

TABLE 6 System's transient response parameters of PID/PD-PI /PD-(1+PI) controllers tuned with MPA technique under case 3

Disturbance		System's transient response parameters									ITAE
		Undershoot (p.u)			Overshoot (p.u)			Settling time (s)			
At $t = 0$ $\Delta P_L = 0.1$ $\Delta \Phi = 200$ W/m^2 at $t = 10$ s and $\Delta \Phi = 100$ W/m^2 at $t = 20$ s		ΔF_1 $\times 10^{-3}$	ΔF_2 $\times 10^{-3}$	ΔP_{tie} $\times 10^{-3}$	ΔF_1 $\times 10^{-3}$	ΔF_2 $\times 10^{-3}$	ΔP_{tie} $\times 10^{-3}$	ΔF_1	ΔF_2	ΔP_{tie}	
Controller	MPA PID	−6.09	−6.56	−21.8	4.60	8.625	11.62	22.97	28.3	30.78	3.635
	MPA PD-PI	−4.47	−1.34	−7.34	2.37	2.039	4.41	22.94	26.4	29.3	1.757
	MPA PD-(1+PI)	−2.23	−0.218	−5.61	1.32	1.687	4.284	22.52	26.13	28.41	1.702

Convergence curves can be used to evaluate the MPA's progress towards minimising the objective function. Figure 5 depicts the progress of MPA in minimising the objective function for various controllers.

5 | APPLICATION OF MPA FOR FREQUENCY CONTROL PROBLEM IN MMG SYSTEM

5.1 | Case1: Fluctuation in load with no change in solar and wind power

Under this condition a step load perturbation (SLP) of 0.1 is applied at $t = 0$ s in microgrid-1 and the step load perturbation of 0.05 in microgrid-2. There is no change in wind speed and solar irradiance. Various recent algorithms along with the

proposed algorithm like GA, DE, GWO and MPA are applied with classical PID controller, cascaded PD-PI controller and the proposed PD-(1+PI) controller to obtain the optimized parameters for each controller which is displayed in Table 1. The ITAE value reported in Table 1 shows that PD-(1+PI) controller gives better result when compared with PID and cascaded PD-PI controller with all the techniques which are chosen for optimization. Further Table 1 reveals that MPA is giving the best result for PID, PD-PI and PD-(1+PI) controller.

Table 2 shows the transient response parameter values for PID controller when optimized with algorithms like GA, DE, GWO, and MPA. Figure 6 shows the MMG's dynamic response comparison of system under case 1 (GA/DE/GWO/MPA) with employing controller PID. For ΔF_1 the undershoot value is $(6.6/14.9/7.91) \times 10^{-3}$ for GA, DE and GWO respectively whereas when tuned with MPA technique it is 6.4×10^{-3} which is least in the considered techniques. Similarly when overshoot

TABLE 7   Transient response parameters of PID/PD-PI /PD-(1+PI) controllers tuned with MPA technique under case-4

Disturbance	Studied controller	Transient response parameters									ITAE
		Undershoot (p.u)			Overshoot (p.u)			Settling time (s)			
SLP = 0.2 p.u. at $t=5$ s		ΔF_1	ΔF_2	ΔP_{tie}	ΔF_1	ΔF_2	ΔP_{tie}	ΔF_1	ΔF_2	ΔP_{tie}	
SLP = 0.4 p.u. at $t=15$ s		$\times 10^{-3}$	$\times 10^{-3}$	$\times 10^{-3}$	$\times 10^{-3}$	$\times 10^{-3}$	$\times 10^{-3}$				
	MPA PID	−8.920	−4.10	−21.5	4.96	10.02	1.55	54.86	56.01	58.78	7.732
SLP = 0.2 p.u at $t=25$ s	MPA PD-PI	−15.95	−1.134	−14.7	2.04	2.45	1.49	52.44	53.81	56.94	2.888
SLP = 0.1 p.u at $t=35$ s with integration of renewable sources	MPA PD – (1+PI)	−5.309	−0.54	−11.1	1.25	1.86	0.47	51.02	51.61	55.56	2.629

TABLE 8   Transient response parameters of PID/PD-PI /PD-(1+PI) controllers tuned with MPA technique under case-5

Controllers	Controller parameters	ITAE
PID	KP1 = 0.8671, KI1 = 4.0001, KD1 = 3.7284,	
	KP2 = -0.0007, KI2 = -0.0370, KD2 = -0.0424 8.022	8.022
PD-PI	KP1 = 3.8121; KI1 = 3.9503; KD1 = -1.2481, KP11 = 1.7747,	4.288
	KP2 = 0.0824; KI2 = -2.0001, KD2 = 0.2682, KP22 = -1.9721	
PD-(1+PI)	KP1 = 4.0001, KI1 = 3.9997, KD1 = 2.4620, KP11 = 0.1741,	
	KP2 = -1.9777, KI2 = 0.0823, KD2 = -1.9077, KP22 = -0.5624	3.549

TABLE 9   Comparative analysis for various techniques

Method/controller	Settling time (T_s) in s			Undershoot (U_s) -ve			ITAE
	ΔF_1	ΔF_2	ΔP_{tie}	ΔF_1	ΔF_2	ΔP_{tie}	
GA: PI [39]	10.3	10.3	9.3	0.23	0.19	0.07	2.7475
BFOA: PI [39]	5.5	7.1	6.35	0.27	0.23	0.08	1.8379
hBFOA-PSO-PI [40]	6.2	6.6	5.73	0.24	0.21	0.071	1.1865
hPSO-PS-Fuzzy PI [41]	4.07	5.25	4.01	0.07	0.035	0.012	0.1438
Proposed MPA: PD-(1+PI)	1.77	4.34	3.67	0.074	0.03	0.010	0.0662

is considered it is $(8.6/8.042/5.124) \times 10^{-3}$ for GA, DE, GWO techniques respectively whereas for MPA it is 4.56×10^{-3} which is better than all other techniques.

To prove the proposed MPA is better than the considered algorithms like GA, DE, GWO, along with PID controller, the cascaded PD-PI controller and proposed PD-(1+PI) controllers are taken and their parameters are tuned with all the above algorithm. The of the system's transient response parameters under investigation using cascaded PD-PI controller tuned with GA\DE\GWO\MPA are collected in Table 3 and showcased in Figure 7 and involving suggested PD-(1+PI) controller optimized with above four algorithm are collected in Table 4 and displayed in Figure 8. From Table 3, it can be witnessed that the undershoot, overshoot and settling time for $\Delta F_1/ \Delta F_2/ \Delta P_{tie}$ are $(-2.33/-1.05/-7.57) \times 10^{-3}$, $(1.30/1.99/0) \times 10^{-3}$, $(4.23/4.21/8.6)$ s respectively when PD-PI controller is tuned with MPA which is better than GA, DE, GWO tuned PD-PI controller.

5.2 | Case 2: Load change with change in wind speed

In this condition, a load change of 0.1 at $t = 0$ is applied to microgrid-1 along with the change in wind speed is employed from 7.5 to 12 m/s at $t = 5$ s and again dropped to 10 m/s from 12 m/s at $t = 15$ s. Change in solar irradiance considered here is zero. Figure 9 exhibits the frequency deviation in microgrids 1 and 2 and the tie-line power and Table 5 displays the transient characteristics of system under investigation under second condition.

5.3 | Case 3: Load change with change in solar irradiance

In this case a step load perturbation of 0.1 is applied at $t = 0$ s is applied to microgrid-1 and the solar irradiation is
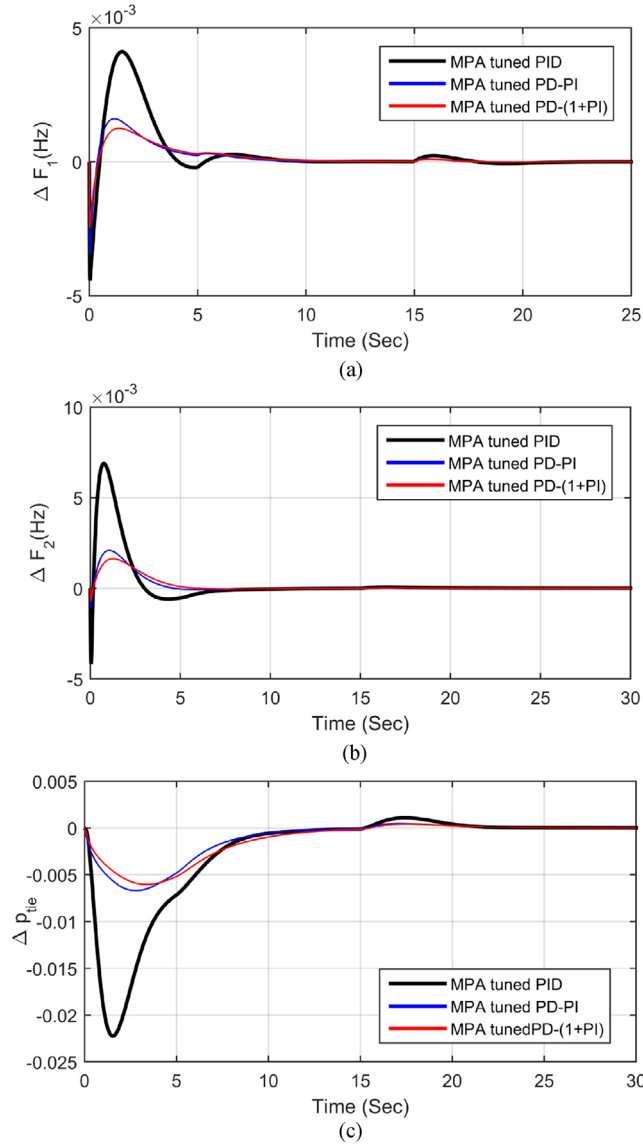
FIGURE 9 Change in frequency and tie-line power under case 2 (a) ΔF_1 in microgrid-1 (b) ΔF_2 in microgrid 2 (c) ΔP_{tie}

$500 \, \text{W/m}^2$. At $t = 10$ s the solar irradiation changed from 500 to $300 \, \text{W/m}^2$ and at $t = 20$ s the change in irradiation is $100 \, \text{W/m}^2$ in the second microgrid. Figure 10 gives the profile of ΔF_1, ΔF_2 and ΔP_{tie} and Table 6 provides the undershoot, overshoot and settling time of the system displayed under case 3.

5.4 | Case 4: When all variations are considered

In this case multi step load perturbation is considered along with change in wind speed and changes in solar irradiance are considered. All the three controllers PID, PD-PI and PD-(1+PI) are employed in the MMG system and its parameters are tuned using MPA. The ITAE value obtained for PID is 7.732 and with PD-PI controller the ITAE value is reduced to 2.888 and is least when PD-(1+PI) controller is used and its
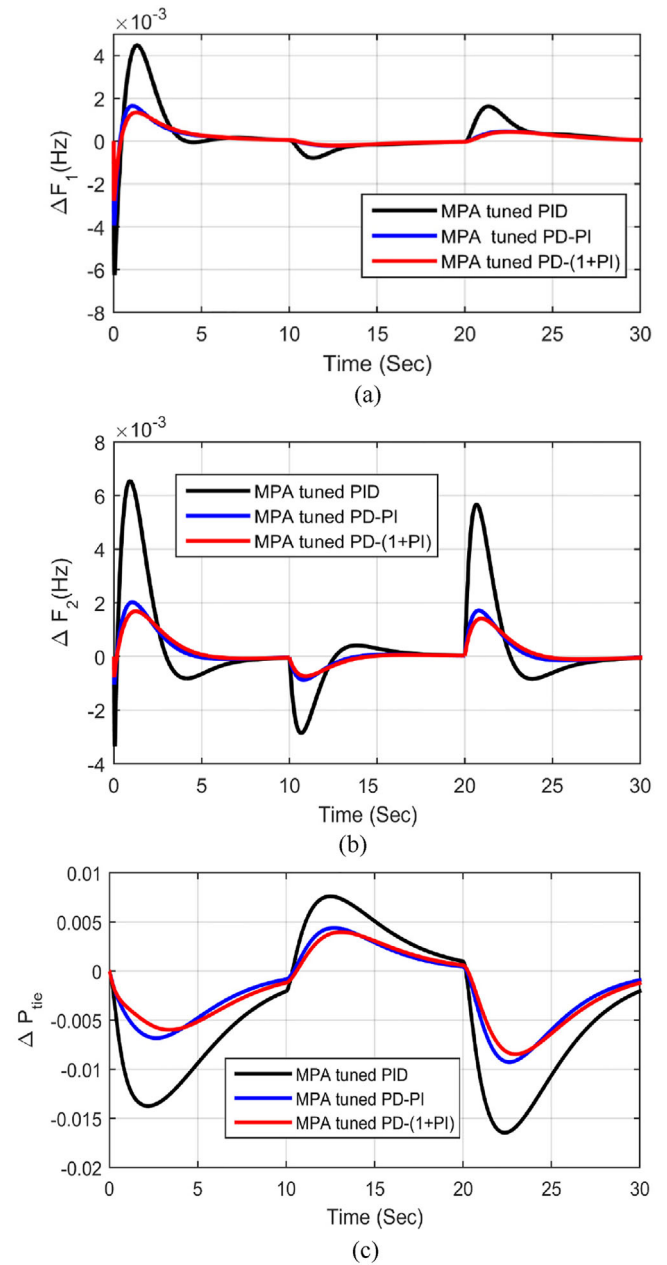

FIGURE 10 Change in frequency and tie-line power under case 3. (a) ΔF_1 in microgrid-1 (b) ΔF_2 in microgrid-2 (c) ΔP_{tie}

value is 2.629 which is collected in Table 7 and the dynamic response parameters are displayed for ΔF_1, ΔF_2, and ΔP_{tie} in Figure 11 claims that the PD-(1+PI) controller gives improved performance than PID controller as well as PD-PI controller.

5.5 | Case-5: Microgrid with non-linearity

In the MMG system, the storage element like BESS and generating unit like DEG has been considered. As it is having renewable sources like WTG and PV cell whose generation are stochastic in nature so it may cause sudden frequency fluctuation. During this disturbance the devices undergo
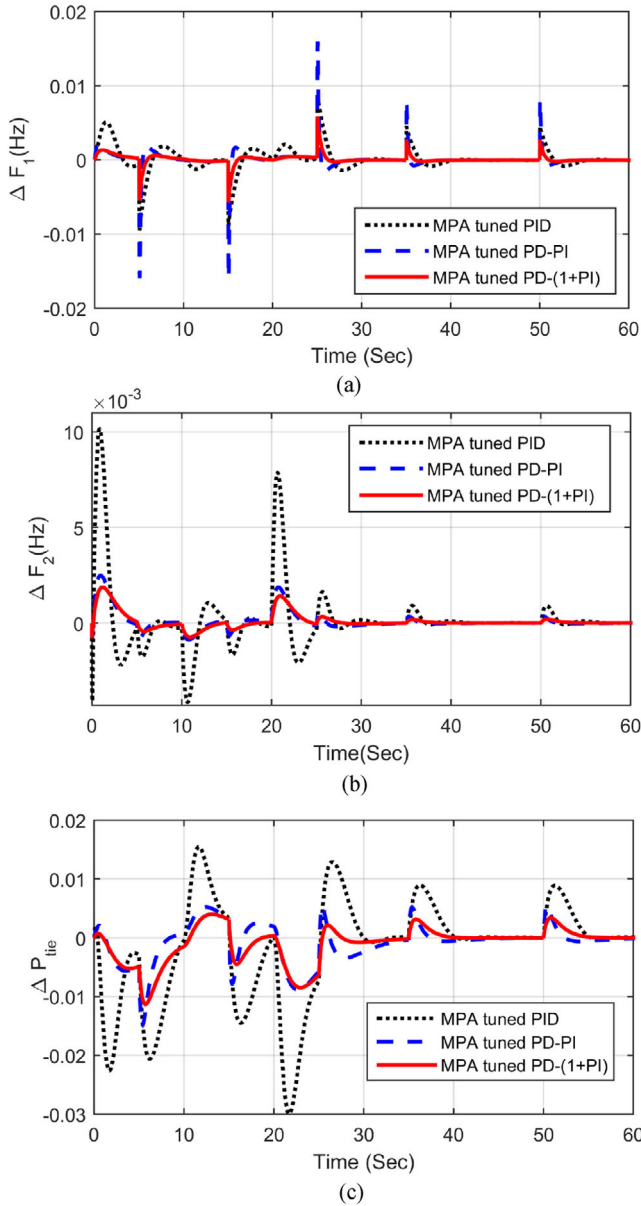
FIGURE 11 Change in frequency and tie line power under case 4 (a) ΔF_1 in microgrid-1 (b) ΔF_2 in microgrid-2 (c) ΔP_{tie}

FIGURE 12 Change in frequency and tie line power under case 5 (a) ΔF_1 in microgrid-1 (b) ΔF_2 in microgrid-2 (c) ΔP_{tie}

electromechanical constraints which can be avoided by using the rate limiter non-linearity. But this causes the storage device and generating unit to operate in a non-linear region.

Here in this case, the rate constraint non-linearity has been chosen for BESS and DEG of microgrid-1. The assumed constraints are $|P\_BESS| < 0.0001$ and $|P\_DEG| < 0.1$. This non-linear environment makes the situation a real one and the proposed controller PD-(1+PI) controller along with the conventional controllers like PID and PD-PI controllers are considered in the MMG with nonlinearity and the ITAE values are found out. The disturbance considered are the load change and change in wind speed which was taken in case 3. The ITAE value along with the controller parameters are collected in Table 8 which says the PID is having a ITAE value of 8.022. When PD-PI controller is
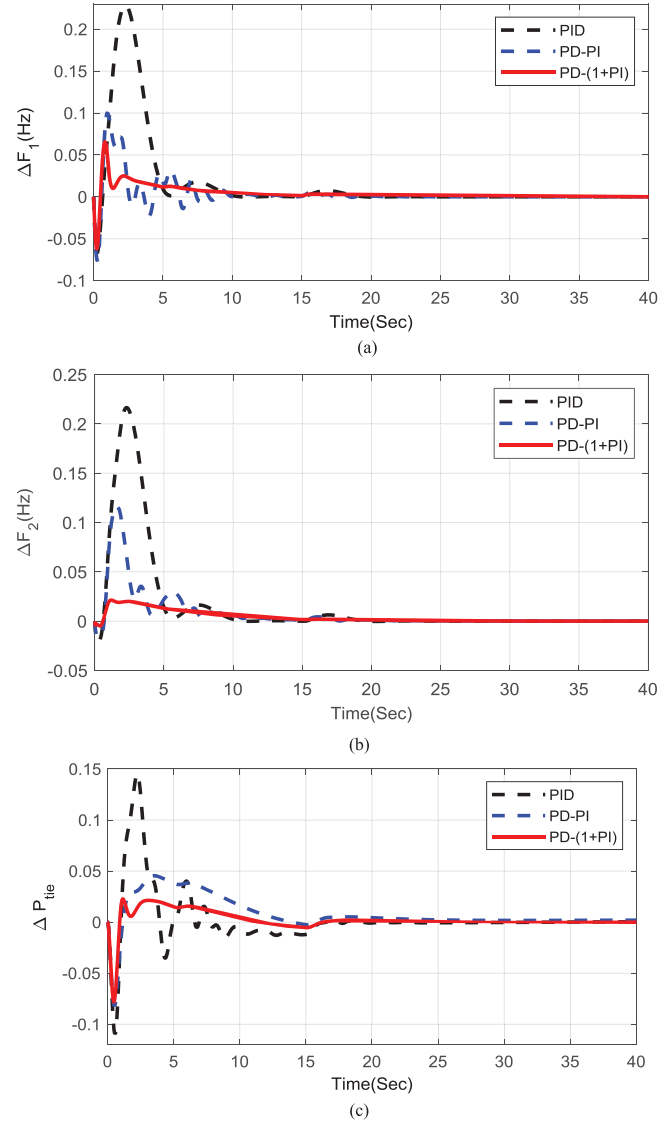
chosen, it reduces the ITAE value to 4.288 and with the proposed PD-(1+PI) controller further reduces the ITAE value to 3.549. The graphs for the frequency deviation of MG1 and MG2 along with the tie-line power are displayed in Figure 12.

5.6 | Case-6: Comparison with recent AGC technique

The proposed frequency control approach is applied to a widely used two-area power system to demonstrate its benefits [39, 40, 41]. In each area, two identical PD-(1+PI) controllers are used. At $t = 0$ s, a 10% sudden disturbance is induced in area 1. The MPA approach is used to tune the parameters of the PD-(1+PI) controller, and its effectiveness is compared to that of various recent optimization techniques
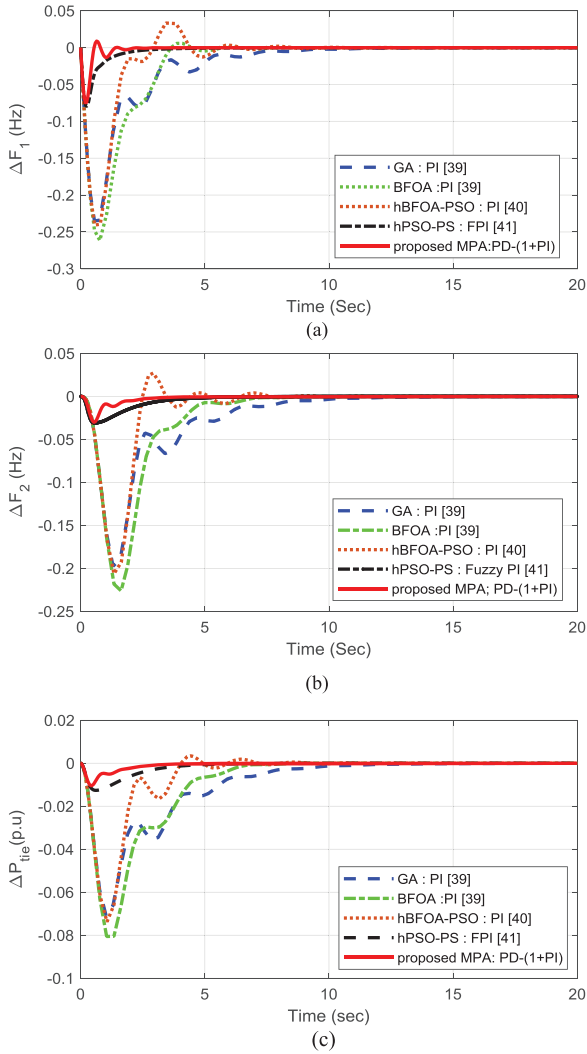
FIGURE 13   Change in frequency and tie line power under case 6 (a) $\Delta F1$ in microgrid-1 (b) ΔF_2 in microgrid-2 (c) ΔP_{tie}

FIGURE 14   Bode responses of MMG system (a) MG1 (b) MG2

as BFOA & GA tuned PI [39], hBFOA-PSO tuned PI [40], and hPSO-PS tuned Fuzzy PI [41], with the results shown in Table 9.

The MPA tuned PD-(1+PI) parameters are: KP1 = 1.9898; KI1 = 1.9900; KD1 = 0.6023; KP11 = 0.3082; KP2 = 0.6257; KI2 = 1.9891; KD2 = 0.4819; KP22 = 1.0796;

Table 9 demonstrates that the MPA-tuned PD-(1+PI) controller achieves the lowest settling time (T_s), Undershoot (U_s) and ITAE value. The MPA-tuned PD-(1+PI) controller outperformed other automatic generation control methods, as shown in Figure 13.

5.7 | Case 7: Bode analysis

The open loop transfer function of the MG1 is given by $G_1(s)$ and the open loop transfer function for MG2 in the MMG system is given by $G_2(s)$. The open loop transfer function for both the MG are 8th order system, and they can be mathematically
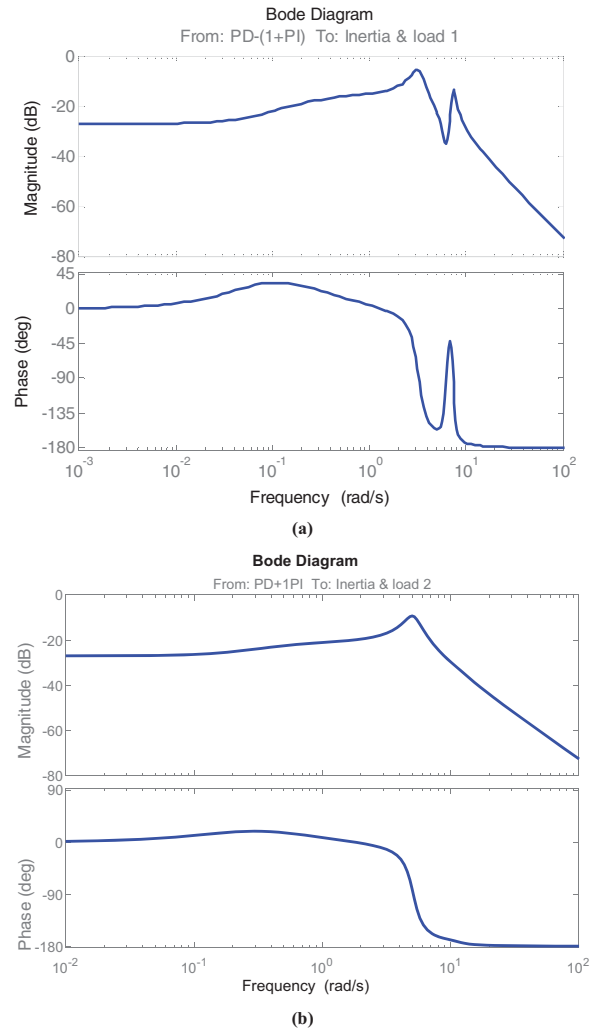

FIGURE 15   Experimental setup based on OPAL-RT

expressed as below. The frequency response is calculated by taking the bode plot of MG1 and MG2. The Figure 14 shows the bode response of MPA tuned PD-(1+PI) controller. It depicts a stable system though the system is going through severe disturbances like fluctuation in load, change in wind power and also the non-linearities. This makes the system a non-linear one.
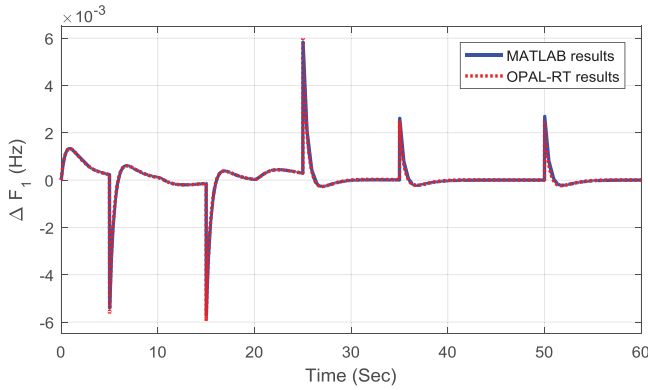
FIGURE 16 Comparison of OPAL-RT Vs MATLAB results showing ΔF_1 in microgrid-1 for case 4

So, the model has been linearized and the response has been taken by taking the input at controller output and output is measured at the output of power system. The gain margin and phase margin are calculated for both the MG and it comes as infinity which indicates the system is stable with the proposed PD-(1+PI) controller.

(1+PI) controller. The transient response parameters collected for various disturbances with PID, cascaded PD-PI controller, PD-(1+PI) controller supports the claim about the superiority of the suggested controller. Considering disturbances in renewable sources along with load change in MMG system, the MPA tuned proposed controller gives least ITAE value when compared with some popular algorithm like genetic algorithm, differential evolution, and grey wolf optimizer. The % decrease in ITAE value with MPA tuned proposed controller compared with some popular algorithm like genetic algorithm, differential evolution, and grey wolf optimizer are 46.29%, 40.05%, and 2.92% respectively. The MPA optimised PD-(1+PI) controller, on the other hand, provides outstanding robustness, faster, more stable, and improved outcomes for a wide range of renewable source unpredictability, and load disturbances. The % decrease in ITAE value with proposed MPA tuned PD-(1+PI) controller compared with MPA tuned PD-PI controller and PID controller are 9%, and 66% respectively considering all variations. All these information affirms the claim that the MPA tuned PD-(1+PI) controller performs efficiently in the MMG system. Finally, OPAL-RT based simulations in a real-time environment are used to validate the proposed MPA-tuned PD-(1+PI) controller in a MMG system.

$$G_1\ (s) = \frac{-2.333s^6 - 50.82s^5 - 379.4s^4 - 1920s^3 - 9226s^2 - 4732s - 348.1}{s^8 + 22.2s^7 + 205.5s^6 + 1550s^5 + 8567s^4 + 1.915e04s^3 + 5.356e04s^2 + 3.823e04s + 7768} \tag{28}$$

$$G_2\ (s) = \frac{2.333s^6 + 50.82s^5 - 520.8s^4 - 3346s^3 - 9075s^2 - 1.848e05s - 4.019e04}{s^8 + 22.2s^7 + 266.2s^6 + 2187s^5 + 3030s^4 - 4.969e04s^3 - 2.564e54s^2 - 2.108e06s + 8.969e05} \tag{29}$$

5.8 | Case 8: Experimental validation

The experimental validation by OPAL-RT is performed for the real-time application of the recommended approach as displayed in Figure 15. The OPAL-RT studies include the inherent delays and errors which are eliminated in usual off-line executions [42]. The frequency deviation in area-1 responses of Real-Time Simulator based on OPAL-RT and MATLAB are revealed in Figure 16. It can be observed from Figure 16 that the MATLAB results closely match with OPAL-RT results.

6 | CONCLUSION

In this present study, MPA technique is proposed to tune PD-(1+PI) controller for a MMG system. The performance of the MMG system is verified by considering the intermittent nature of renewable sources and load fluctuations. The dynamic performances of the considered MMG system are compared to the results produced by typical PD-PI and PID controllers to demonstrate the feasibility of the proposed PD-

CONFLICT OF INTEREST

No potential conflict of interest was reported by authors.

ORCID

Sanjeevikumar Padmanaban https://orcid.org/0000-0003-3212-2750
Baseem Khan https://orcid.org/0000-0002-5082-8311

REFERENCES

1. Rajesh, K.S., Dash, S.S., Rajagopal, R., Sridhar, R.: A review on control of ac microgrid. Renewable Sustainable Energy Rev. 71, 814—819 (2017)
2. Ahmad, F., Alam, M.S., Shahidehpour, M.: Profit maximization of microgrid aggregator under power market environment. IEEE Syst. J. 13(3), 3388—3399 (2018)
3. Shuai, Z., Sun, Y., Shen, Z.J., Tian, W., Tu, C., Li, Y., Yin, X.: Microgrid stability: Classification and a review. Renewable Sustainable Energy Rev. 58, 167—179 (2016)
4. Olivares, D.E., Mehrizi-Sani, A., Etemadi, A.H., Cañizares, C.A., Iravani, R., Kazerani, M., Hajimiragha, A.H., Gomis-Bellmunt, O., Saeedifard, M., Palma-Behnke, R., Jiménez-Estévez, G.A.: Trends in microgrid control. IEEE Trans. Smart Grid. 5(4), 1905—1919 (2014)
5. Mehrizi-Sani, A., Iravani, R.: Potential-function based control of a microgrid in islanded and grid-connected modes. IEEE Trans. Power Syst. 25(4), 1883—1891 (2010)

6. Jiang, Q., Xue, M., Geng, G.: Energy management of microgrid in grid-connected and stand-alone modes. IEEE Trans. Power Syst. 28(3), 3380––3339 (2013)

7. Singh, K., Amir, M., Ahmad, F., Khan, M.A.: An integral tilt derivative control strategy for frequency control in multimicrogrid system. IEEE Syst. J. 15(1), 1477–88 (2020)

8. Sahoo, S.K., Sinha, A.K., Kishore, N.K.: Control techniques in AC, DC, and hybrid AC–DC microgrid: A review. IEEE Trans. Emerging Sel. Top. Power Electron. 6(2), 738–759 (2017)

9. Shankar, R., Pradhan, S.R., Chatterjee, K., Mandal, R.: A comprehensive state of the art literature survey on LFC mechanism for power system. Renewable Sustainable Energy Rev. 76, 1185—207 (2017)

10. Mallesham, G., Mishra, S., Jha, A.N.: Ziegler-Nichols based controller parameters tuning for load frequency control in a microgrid. In: 2011 International Conference on Energy, Automation and Signal, Bhubaneswar, India, pp. 1—8 (2011)

11. Dhanalakshmi, R., Palaniswami, S.: Load frequency control of wind diesel hydro hybrid power system using conventional PI controller. Eur. J. Sci. Res. 19(7), 630–641 (2011)

12. Vidyanandan, K.V., Senroy, N.: Frequency regulation in a wind–diesel powered microgrid using flywheels and fuel cells. IET Gener. Transm. Distrib. 10(3), 780–788 (2016)

13. Ray, P.K., Mohanty, S.R., Kishor, N.: Proportional–integral controller based small-signal analysis of hybrid distributed generation systems. Energy Convers. Manage. 52(4), 1943–1954 (2011)

14. Pandey, A., Tyagi, N.: Frequency control of an autonomous hybrid generation system. In: 2017 IEEE International Conference on Power, Control, Signals and Instrumentation Engineering (ICPSI), Chennai, India, pp. 2688—2693 (2017)

15. Veronica, A.J., Kumar, N.S.: Internal model-based load frequency controller design for hybrid microgrid system. Energy Procedia. 117, 1032—1039 (2017)

16. Lal, D.K., Barisal, A.K.: Load frequency control of AC microgrid interconnected thermal power system. IOP Conf. Ser.: Mater. Sci. Eng. 225(1), 012090 (2017)

17. Kumar, R.H., Ushakumari, S.: Biogeography based tuning of PID controllers for load frequency control in microgrid. In: 2014 International Conference on Circuits, Power and Computing Technologies [ICCPCT-2014], Nagercoil, India, pp. 797—802 (2014)

18. Gupta, E., Saxena, A.: Grey wolf optimizer-based regulator design for automatic generation control of interconnected power system. Cogent Eng. 3(1), 1151612 (2016)

19. Sahu, R.K., Panda, S., Padhan, S.: Optimal gravitational search algorithm for automatic generation control of interconnected power systems. Ain Shams Eng. J. 5, 721–733 (2015)

20. Guha, D., Roy, P., Banerjee, S.: Study of differential search algorithm based automatic generation control of an interconnected thermal-thermal system with governor dead band. Appl. Soft Comput. 52, 160–175 (2017)

21. Arya, Y.,: Effect of energy storage systems on automatic generation control of interconnected traditional and restructured energy systems. Int. J. Energy Res. 43(12), 6475–6493 (2019)

22. Patel, S., Mohanty, B., Hasanien, H.M.: Competition over resources optimized fuzzy TIDF controller for frequency stabilization of hybrid micro-grid system. Int. Trans. Electr. Energy Syst. 30(9), e12513 (2020)

23. Nayak, P.C., Prusty, U.C., Prusty, R.C., Panda, S.: Imperialist competitive algorithm optimized cascade controller for load frequency control of multi-microgrid system. Energy Sources Part A. 28, 1–23 (2021)

24. Nayak, P.C., Bisoi, S., Prusty, R.C., Panda, S.: Performance analysis of PDF+ (1+ PI) controller for load frequency control of the multi microgrid system using genetic algorithm. In: 2019 International Conference on Information Technology (ICIT),Bhubaneswar,India, pp. 448–453 (2019)

25. Kumar Khadanga, R., Kumar, A., Panda, S.: Frequency control in hybrid distributed power systems via type-2 fuzzy PID controller. IET Renewable Power Gener. 15(8), 1706–23 (2021)

26. Gorripotu, T.S., Ramana, P., Sahu, R.K., Panda, S.: Sine cosine optimization based proportional derivative-proportional integral derivative controller for frequency control of hybrid power system. In: Computational Intelligence in Data Mining, pp. 789–797, Springer, Singapore (2020)

27. Sahu, R.K., Panda, S., Rout, U.K., Raul, P.: Application of gravitational search algorithm for load frequency control of multi area power system. J. Bioinf. Intell. Control 2(3), 200–210 (2013)

28. Arya, Y.: AGC of PV-thermal and hydro-thermal power systems using CES and a new multi-stage FPIDF-(1+ PI) controller. Renewable Energy 134, 796–806 (2019)

29. Arya, Y., Dahiya, P., Çelik, E., Sharma, G., Gözde, H., Nasiruddin, I.: AGC performance amelioration in multi-area interconnected thermal and thermal-hydro-gas power systems using a novel controller. Eng. Sci. Technol. Int. J. 24(2), 384–396 (2021)

30. Arya, Y., Kumar, N., Dahiya, P., Sharma, G., Çelik, E., Dhundhara, S., Sharma, M.: Cascade-IλDμN controller design for AGC of thermal and hydro-thermal power systems integrated with renewable energy sources. IET Renewable Power Gener. 15(3), 504–520 (2021)

31. Sharma, M., Dhundhara, S., Arya, Y., Prakash, S.: Frequency excursion mitigation strategy using a novel COA optimised fuzzy controller in wind integrated power systems. IET Renewable Power Gener. 14(19), 4071–4085 (2020)

32. Celik, E., Öztürk, N., Arya, Y., Ocak, C.: (1+ PD)-PID cascade controller design for performance betterment of load frequency control in diverse electric power systems. Neural Comput. Appl. 33(22), 15433–15456 (2021)

33. Dahiya, P., Mukhija, P., Saxena, A.R., Arya, Y.: Comparative performance investigation of optimal controller for AGC of electric power generating systems. Automatika: časopis za automatiku, mjerenje, elektroniku, računarstvo i komunikacije. 57(4), 902–921 (2016)

34. Pradhan, C., Bhende, C.N.: Online load frequency control in wind integrated power systems using modified Jaya optimization. Eng. Appl. Artif. Intell. 77, 212–228 (2019)

35. Xu, Y., Zhou, J., Xue, X., Fu, W., Zhu, W., Li, C.: An adaptively fast fuzzy fractional order PID control for pumped storage hydro unit using improved gravitational search algorithm. Energy Convers. Manage. 111, 67–78 (2016)

36. Kler, D., Kumar, V., Rana, K.P.: Optimal integral minus proportional derivative controller design by evolutionary algorithm for thermal-renewable energy-hybrid power systems. IET Renewable Power Gener. 13(11), 2000–2012 (2019)

37. Faramarzi, A., Heidarinejad, M., Mirjalili, S., Gandomi, A.H.: Marine Predators Algorithm: A nature-inspired meta-heuristic. Expert Syst. Appl. 152, 113377 (2020)

38. Filmalter, J.D., Dagorn, L., Cowley, P.D., Taquet, M.: First descriptions of the behavior of silky sharks, Carcharhinus falciformis, around drifting fish aggregating devices in the Indian Ocean. Bull. Mar. Sci. 87(3), 325–337 (2011)

39. Ali, E.S., Abd-Elazim, S.M.: Bacteria foraging optimization algorithm-based load frequency controller for interconnected power system. Int. J. Electr. Power Energy Syst. 33, 633–638 (2011)

40. Sahu, R.K., Panda, S., Sekher, G.T.C.: A novel hybrid PSO-PS optimized fuzzy PI controller for AGC in multi area interconnected power systems. Int. J. Electr. Power Energy Syst. 64, 880–893 (2015)

41. Panda, S., Mohanty, B., Hota, P.K.: Hybrid BFOA-PSO algorithm for automatic generation control of linear and nonlinear interconnected power systems. Appl. Soft Comput. 13, 4718–4730 (2013)

42. Khooban, M.H.: Secondary load frequency control of time-delay stand-alone micro-grids with electric vehicles. IEEE Trans. Ind. Electron. 65(9), 7416–7422 (2017)